

Non-equilibrium effects and spherocity in relativistic proton-nucleus collisions

L. OLIVA⁽¹⁾⁽²⁾, W. FAN⁽³⁾, P. MOREAU⁽³⁾, S. A. BASS⁽³⁾
and E. BRATKOVSKAYA⁽⁴⁾⁽⁵⁾⁽⁶⁾

⁽¹⁾ *Department of Physics and Astronomy “Ettore Majorana”, University of Catania
Via S. Sofia 64, I-95123 Catania, Italy*

⁽²⁾ *INFN Sezione di Catania - Via S. Sofia 64, I-95123 Catania, Italy*

⁽³⁾ *Department of Physics, Duke University - Durham, NC 27708, USA*

⁽⁴⁾ *Helmholtz Research Academy Hesse for FAIR (HFHF), GSI Helmholtz Center for Heavy
Ion Physics, Campus Frankfurt - 60438 Frankfurt, Germany*

⁽⁵⁾ *Institut für Theoretische Physik, Johann Wolfgang Goethe-Universität
Max-von-Laue-Str. 1, D-60438 Frankfurt am Main, Germany*

⁽⁶⁾ *GSI Helmholtzzentrum für Schwerionenforschung GmbH - Planckstrasse 1,
D-64291 Darmstadt, Germany*

received 23 July 2024

Summary. — We examine nonequilibrium dynamics in proton-nucleus collisions at LHC energy by comparing the Parton-Hadron-String-Dynamics (PHSD) transport approach with the (2+1)dimensional viscous hydrodynamic model VISHNew. The latter is initialized with initial conditions extracted from PHSD. We observe that PHSD exhibits highly inhomogeneous energy density profiles on the transverse plane throughout the evolution, while VISHNew efficiently smooths initial spatial irregularities yet maintains significant inhomogeneity due to the smaller space-time size of the medium produced in small systems compared to heavy-ion reactions. The two approaches present also a very different evolution of the bulk viscous pressure. Furthermore, we analyze transverse spherocity distribution in PHSD and the hybrid approach (VISHNew + hadronic afterburner). We find a shift towards isotropic event configurations in PHSD compared to the result of the hybrid model. This dissimilarity should primarily arise from the different descriptions of the medium within the two frameworks. We support the utility of multi-differential measurements based on multiplicity and spherocity selection for studying final-state observables in relativistic proton-nucleus collisions.

1. – Introduction

High-energy nuclear collisions at the Relativistic Heavy Ion Collider (RHIC) and the Large Hadron Collider (LHC) are aimed at accessing experimentally hot QCD matter. Besides strong evidences of the formation of Quark-Gluon Plasma (QGP), a deconfined state of quarks and gluons, in relativistic heavy-ion collisions, more recently QGP signals

emerged also in high-multiplicity proton-proton (pp) and proton-nucleus (pA) collisions, suggesting the formation of short-lived QGP droplets also in these small systems [1].

Two theoretical approaches have been developed in the last decades to successfully describe the dynamical evolution of the hot QCD medium produced in relativistic nuclear collisions, both large and small systems: hydrodynamic models are based on a macroscopic description of the system in which the evolution is governed by conservation laws (such as those for the energy-momentum tensor and the baryon current) [2,3]; transport approaches give a microscopic description of the interacting many-body system in which the evolution is governed by kinetic equations for the elementary degrees-of-freedom [4]. An approximate local equilibrium was traditionally considered a necessary condition for the validity of viscous hydrodynamics, until it turned out to be successful to describe the experimental measurements in small systems, where the medium is probably quite far from local equilibrium. This has triggered several studies of hydrodynamic attractors for understanding the onset of the regime where hydrodynamics is applicable [5,6]. The transport approach is a nonequilibrium dynamical model, hence it is inherently suited for describing off-equilibrium processes like those affecting small system collisions or the very early stages of heavy-ion collisions. The emergence of the universal attractor behavior has been studied also by means of transport simulation models based on the kinetic Boltzmann equation with the full collision integral [7,8]. Within the transport approach it is possible to model the collision since the early times when the two nuclei approach one each other and it is able to describe not only the partonic phase but also the hadronic one. Hydrodynamic simulations start with some given initial conditions and after the hadronization stage the evolution in the hadronic phase is demanded to a so-called hadronic afterburner based on the kinetic description.

This work focuses on the evolution of the medium produced in proton-nucleus collisions [9], in particular the $p + \text{Pb}$ collisions at $\sqrt{s_{NN}} = 5.02$ TeV performed at LHC, by comparing the Parton-Hadron-String Dynamics (PHSD) transport approach [10-12] and the VISHNew viscous hydrodynamic model [13,14]. Initial conditions for the hydrodynamic model are extracted from PHSD, which describes the full space-time evolution of relativistic nuclear collisions, from initial hard scatterings through the deconfined QGP phase to the subsequent hadronic stage. This investigation aims to highlight the nonequilibrium traces in the medium evolution of small systems. A similar analysis has been performed in ref. [15] for the case of relativistic heavy-ion collisions and the investigation of the non-equilibrium effects has been extended to heavy quark dynamics in ref. [16]. Furthermore, the present work explores event-shape analysis with transverse sphericity [17-19] in proton-nucleus collisions [9], a method that distinguishes events based on their topology and may help to identify QGP signals in small systems [20].

2. – Dynamical description of relativistic nuclear collisions

The two approaches used in the present work to simulate the dynamical evolution of proton-nucleus collisions are described in detail in Refs. [9,15] and references therein. Here we summarize the main ingredients.

2.1. The PHSD transport approach. – PHSD is a covariant dynamical framework for strongly interacting many-body systems, founded on generalized transport equations derived from off-shell Kadanoff-Baym theory for non-equilibrium Green functions [10,11]. These equations allow to comprehensively describe the time evolution of both partonic and hadronic phases. PHSD simulations span the entire space-time history of nuclear

collisions, starting from the initial nucleon-nucleon inelastic scatterings between the colliding nuclei, extending through the QGP phase formed when the local energy density surpasses the deconfinement transition value and subsequent hadronization as well as describing the evolution and interactions within the hadronic phase. The QGP properties are described with the Dynamical Quasi-Particle Model (DQPM) [11], which defines parton spectral functions with parameters determined via the lattice QCD Equation of State (EoS). The specific shear viscosity η/s and bulk viscosity ζ/s of the QGP are extracted from the partonic interaction rates in the DQPM and agree with lattice QCD calculations [21, 22]. Additionally, a dynamical hadronization process accounts for the merging of off-shell quarks and antiquarks into off-shell hadrons [11, 12].

2.2. The hybrid model: hydrodynamics plus hadronic afterburner. – This hybrid framework [13] combines the boost-invariant relativistic 2+1 dimensional viscous hydrodynamic model VISHNew [14] with the microscopic Ultrarelativistic Quantum Molecular Dynamics (UrQMD) model [23, 24] to simulate different phases of nuclear collisions. VISHNew simulates the hot and dense QGP phase by means of the conservation equations for the energy-momentum tensor $T^{\mu\nu}$ of the hydrodynamic fluid. The time evolution of viscous corrections is determined through second-order Israel-Stewart equations in the 14-momentum approximation [25]. In order to initialize the hydrodynamic equations, the profiles on the transverse plane of the fluid flow velocity u^μ , the energy density e , the equilibrium pressure P , the bulk viscous pressure Π and the shear stress tensor $\pi^{\mu\nu}$ are extracted from PHSD using a Landau matching procedure [9, 15]. The bulk viscosity adopted in VISHNew is determined via the Bayesian analysis of the available experimental data [26], while the shear viscosity used in the present work is given by a parametrization of the $\eta(T)/s$ extracted from PHSD [15]. The hydrodynamic equations are closed using an EoS derived from lattice QCD calculations and subsequently merged with a hadron resonance gas EoS [13], obtaining a EoS in line with the one reproduced by the DQPM in PHSD. Below a certain temperature, the transition from the hydrodynamic medium into particles is realized via a Cooper-Frye algorithm. The formed hadronic matter evolves microscopically using the UrQMD model [23, 24].

3. – Nonequilibrium evolution of the hot and dense viscous medium

The time evolution of the hot and dense medium produced is ultrarelativistic proton-nucleus collisions is studied by investigating the response of the hydrodynamic long-wavelength evolution to the PHSD initial conditions and comparing with the nonequilibrium PHSD evolution. The initial conditions for the hydrodynamic simulation are extracted by coarse-graining the PHSD medium at three different times t_0 ; here we show results obtained starting the hydrodynamic evolution at $t_0 = 0.2$ fm/c and $t_0 = 0.4$ fm/c. The flow and viscous corrections determined from PHSD at those times are included in the initial conditions for the VISHNew simulations. The two models share the same initial profiles of macroscopic quantities at t_0 , however the subsequent evolution may be quite dissimilar due to the different dynamics underlying the two approaches.

The energy density decreases quickly as the medium expands. In ref. [9] it has been shown that the energy density profile obtained with PHSD is highly inhomogeneous in the transverse plane during the whole time evolution of the proton-induced collision; while the hot spots are more efficiently dissolved in VISHNew leading to a much smoother energy density profile after t_0 . However, due to the smaller space-time size of the fireball in small systems, the energy density profile maintains a higher degree of inhomogeneity

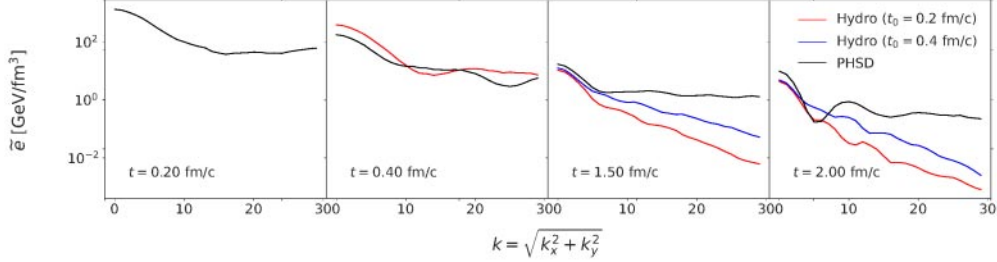


Fig. 1. – Radial distribution of the Fourier modes of the energy density for a single p+Pb collisions at $\sqrt{s_{NN}} = 5.02$ TeV with impact parameter $b = 2$ fm. The black line is obtained with PHSD, while the red and blue curves are from the hydrodynamic simulations started at different initialization times. The four panels show different times of the collision evolution. Figure adapted from ref. [9].

throughout its evolution with respect to heavy-ion reaction [15]. The inhomogeneity of the medium can be quantified by computing the Fourier transform of the energy density. For a discrete spatial grid of size $(L_x, L_y) = (0.1 \text{ fm}, 0.1 \text{ fm})$ with an energy density distribution $e(x, y)_{m \times n}$, the Fourier coefficients are given by

$$(1) \quad \tilde{e}(k_x, k_y) = \frac{1}{m} \frac{1}{n} \sum_{x=0}^{m-1} \sum_{y=0}^{n-1} e(x, y) e^{2\pi i \left(\frac{x k_x}{L_x m} + \frac{y k_y}{L_y n} \right)}.$$

The zeroth mode $\tilde{e}(k_x = 0, k_y = 0)$ is the sum of the energy density values over all grid points, while higher order coefficients tell us how much the local energy density is correlated on different length scales. The Fourier image of the energy density \tilde{e} is depicted in fig. 1 as a function of the k mode at different times. The black curve obtained with the PHSD simulation is compared with the results of the hydrodynamic evolution starting at different initialization times t_0 . In the PHSD case the short wavelength inhomogeneities persist during all time evolution, even though their strength slightly decreases due to the system dilution during the fireball expansion. The excitation of higher-order Fourier modes is inherent to a microscopic nonequilibrium dynamics, such that underlying the PHSD transport approach. In the hydrodynamic evolution, the strength of the Fourier modes is similar to that in PHSD at the early times, but after about 1 fm/c higher-order coefficients are strongly suppressed while the lower Fourier modes dominate. This means that only the global shape of the event in terms of energy density survives and shorter wavelength irregularities are washed out. This is expected considering that the hydrodynamic evolution can only capture the large wavelength structure of the medium. Regarding the effect of the initialization time, higher-order Fourier modes are less suppressed if the hydrodynamic simulation starts at a later time, as can be seen by comparing the blue and red lines; however, their values are still far below those obtained with the microscopic evolution. These results clearly highlight the difference between the two approaches in the treatment of short wavelength irregularities, difference that is even more pronounced in pA collisions [9] with respect to heavy-ion reactions [15].

Besides the energy density, other interesting information comes from the investigation of the evolution of the viscous corrections. We computed the bulk viscous pressure

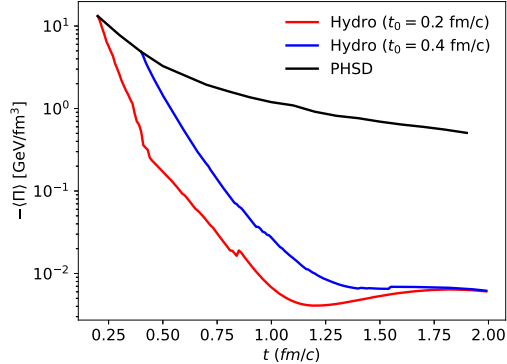


Fig. 2. – Time evolution of the bulk viscous pressure $-\Pi$ weighted by the energy density and averaged over the transverse plane at midrapidity ($z = 0$) for p+Pb collisions at $\sqrt{s_{NN}} = 5.02$ TeV with $b = 2$ fm. The lines are obtained averaging over many events in PHSD (black line) and hydrodynamics with different initialization times (red and blue lines). Figure adapted from ref. [9].

$\Pi = -\text{Tr}(\Delta_{\mu\nu}T^{\mu\nu})/3 - P$, where $\Delta_{\mu\nu}$ is the projector onto the space orthogonal to u^μ . In ref. [9] we have shown that, even though large deviations from equilibrium (quantified with the ratio Π/P) are present both in PHSD and VISHNew at the early times of a pA collision, they are strongly reduced in the hydrodynamic case while persist during the whole microscopic evolution. Nevertheless, some spots where the bulk contribution to pressure is of the same order as the equilibrium one are still present at later times also in the hydrodynamic simulations, supporting the idea that the fireball produced in small colliding systems remain out of equilibrium throughout its dynamical evolution. In fig. 2 we show the absolute value of the event average of $\langle\Pi\rangle$, which is the bulk viscous pressure Π weighted with the energy density e and averaged over the transverse plane:

$$(2) \quad \langle\Pi\rangle = \frac{\int d^2\mathbf{x}_T \Pi(x, y) e(x, y)}{\int d^2\mathbf{x}_T e(x, y)}.$$

The black curve is the PHSD result while the red and blue curves correspond to hydrodynamic simulations initialized at different times from PHSD profiles. The bulk viscous pressure Π is initially very large and negative due to the large expansion rate at initial times. Its magnitude experiences a power-law decay in PHSD simulations; however, $-\langle\Pi\rangle$ presents still a value of about $0.5 \text{ GeV}/\text{fm}^3$ at $t = 2 \text{ fm}/c$, time corresponding roughly to the end of the QGP lifetime in the hydrodynamic evolution. The red and blue lines show that in the hydrodynamic case Π , which has at t_0 the same value as in PHSD due to the initialization, drops thereafter very quickly with respect to PHSD vanishing within about half fm/c . This conspicuous difference between the results within the hydrodynamic and transport approaches is partially due to the temperature dependence of the bulk viscosity, which largely governs the evolution of Π in hydrodynamics. Indeed, in PHSD ζ/s is larger than in VISHNew [15], since the latter cannot handle large bulk viscosities. However, we see that in both cases the evolution of the bulk viscous pressure obtained in pA collisions is quite faster than that found in heavy-ion collisions [27]. It is worth to note that the two curves from hydrodynamic simulations corresponding to different starting times t_0 are very different at the beginning (being them extracted from

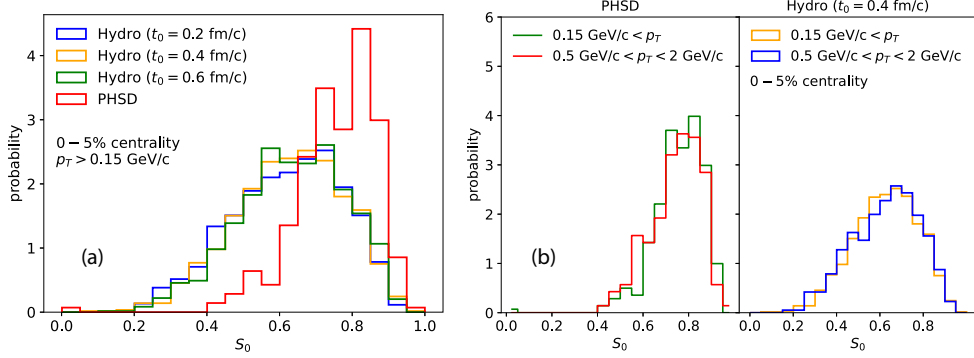


Fig. 3. – Probability distribution of events as a function of sphericity in 5% central p+Pb collisions at $\sqrt{s_{NN}} = 5.02$ TeV. Panel (a) shows PHSD events (red line) and the hybrid model with hydrodynamics starting from PHSD initial conditions at three different times (green, orange and blue curves). Panel (b) shows the effect of selecting particles in different p_T ranges for the computation of S_0 . Figure adapted from ref. [9].

PHSD at t_0) but then converge to the same trajectory within 2 fm/c. This attractor behaviour, seen also in heavy-ion collisions after 1-2 fm/c [27], indicates that there is a loss of memory of the initial conditions concerning the medium viscous correction, which however happens quite late in the fireball evolution [28]; in particular, we see from fig. 2 that the convergence of different curves corresponding to different initial conditions is reached at times close to the end of the QGP evolution in small colliding systems.

4. – Transverse sphericity analysis in proton-nucleus collisions

The challenge of connecting the collective behavior observed in small systems with initial-state effects or recognizing it as a signature of QGP has prompted initial investigations into examining observables associated with particle production and anisotropic flow through multidifferential analysis. This approach involves selecting centrality alongside categorizing events based on their shapes. One of such event-shape selection methods utilized across various colliding system sizes is transverse sphericity analysis. The transverse sphericity, S_0 , is defined as

$$(3) \quad S_0 \equiv \frac{\pi^2}{4} \min_{\hat{\mathbf{n}}_s} \left(\frac{\sum_i |\mathbf{p}_{Ti} \times \hat{\mathbf{n}}_s|}{\sum_i p_{Ti}} \right)^2,$$

with $\hat{\mathbf{n}}_s$ being a unit vector which minimizes the ratio in eq. (3), where the sum runs over all charged particles in selected intervals of pseudorapidity η and transverse momentum p_T ; we choose $|\eta| < 0.5$ and $p_T > 0.15$ GeV/c, as done in experiments. In order to achieve a good sphericity resolution at least three tracks are required within those η and p_T regions. There are two limits for the values of transverse sphericity: $S_0 \rightarrow 0$ corresponds to “jetty” events, where all transverse momentum vectors are (anti)parallel or their sum is dominated by a single track; $S_0 \rightarrow 1$ is obtained for “isotropic” events, where the transverse momentum vectors are isotropically distributed. In pp collisions [29] the jetty configurations are usually the result of hard processes while the isotropic ones are events dominated by soft processes. In fig. 3 we present the normalized distribution of events as a function of transverse sphericity for collisions in the 0-5% centrality class.

In panel (a) the red line is the PHSD result, while blue, yellow and green lines correspond to simulations performed with the hybrid model starting viscous hydrodynamics at three different initial times: $t_0 = 0.2, 0.4, 0.6$ fm/c. The centrality categorization in the hybrid model is done by initializing hydrodynamics from minimum bias PHSD events and then selecting the 5% most central events. We notice that the sphericity distribution in PHSD is shifted more towards the isotropic limit ($S_0 \rightarrow 1$) compared to the hybrid model. The PHSD result is similar to predictions from the AMPT transport approach [19]. The difference between the PHSD and hybrid model is in part due to the different event probability as a function of charged particle multiplicity for the two cases [9], but from a further analysis seems to be more connected to the different dynamics underlying the two approaches. In ref. [30] it has been pointed out that event topology is driven by the underlying particle production dynamics and medium effects. It would be interesting to further investigate the dissimilarity shown in fig. 3(a) by employing a (3+1)dimensional hydrodynamic model. In panel (b) of fig. 3 we show the transverse sphericity distribution of events obtained considering two different transverse momentum cuts when computing S_0 from eq. (3) with charged particles. Even though the event distribution as a function of charged particle multiplicity is substantially modified in both PHSD and hydrodynamics if different p_T cuts are applied [9], we see from fig. 3(b) that the transverse sphericity distribution does not change within the same approach. This supports the idea that the dissimilarity between PHSD and hydrodynamics shown in fig. 3(a) in the sphericity distribution is not strongly related to the difference in the charged particle multiplicity, but is rather related to the underlying description within the two frameworks of the hot and dense medium produced in proton-nucleus collisions. Performing an event-shape analysis with sphericity in pA collisions adds to the collection of such tools that have already been discussed for pp collisions [29, 31, 32].

5. – Conclusions

This study investigates the evolution of the medium formed in small colliding systems and its far-from-equilibrium dynamics using both microscopic transport (PHSD) and macroscopic hydrodynamic (VISHNew) descriptions. Initial conditions for VISHNew are obtained from PHSD, in order to mitigate early out-of-equilibrium effects and emphasize nonequilibrium traces during subsequent medium evolution in p+Pb collisions at LHC energy. The comparison reveals highly inhomogeneous energy density in PHSD, while hydrodynamic simulations dissolve initial hot spots more efficiently but maintain significant inhomogeneity due to the smaller collision system size. Fourier modes of energy density show initially similar strengths but diverge rapidly thereafter, indicating sustained spatial irregularities during the whole microscopic evolution. Bulk viscous pressure exhibits a quicker decay in magnitude in hydrodynamics with respect to PHSD. Hydrodynamic simulations starting at different initialization times converges to a single trajectory, resembling the attractor behavior, at times close to the end of lifetime of QGP medium in small systems. Understanding nonequilibrium effects in proton-nucleus collisions may help in identifying their impact on final observables, particularly those connected to QGP formation. Multi-differential measurements, such as those based on event classification according to multiplicity and topology, may be important tools to study properties of the medium produced in ultra-relativistic proton-nucleus collisions and QGP signals. Our event-shape analysis based on transverse sphericity shows a preference for more isotropic event topologies in PHSD with respect to the hybrid approach that connects the hydrodynamic evolution with an hadronic afterburner. While this dis-

similarity partly stems from differences in final charged particle multiplicity, it mainly arises from the different descriptions of the medium in small colliding systems underlying the two frameworks.

* * *

LO acknowledges the Next Generation action of the European Commission and the MUR funding (PNRR Missione 4) under the HEFESTUS project. SAB, PM and WF acknowledge support from DOE grant no. DE-FG02-05ER41367.

REFERENCES

- [1] NAGLE J. L. and ZAJC W. A., *Annu. Rev. Nucl. Part. Sci.*, **68** (2018) 211.
- [2] ROMATSCHKE P. and ROMATSCHKE U., *Relativistic Fluid Dynamics In and Out of Equilibrium, Cambridge Monographs on Mathematical Physics* (Cambridge University Press) 2019.
- [3] SHEN C. and YAN L., *Nucl. Sci. Tech.*, **31** (2020) 122.
- [4] BLEICHER M. and BRATKOVSKAYA E., *Prog. Part. Nucl. Phys.*, **122** (2022) 103920.
- [5] HELLER M. P. and SPALINSKI M., *Phys. Rev. Lett.*, **115** (2015) 072501.
- [6] STRICKLAND M., NORONHA J. and DENICOL G., *Phys. Rev. D*, **97** (2018) 036020.
- [7] AMBRUS V. E., BUSUIOC S., FOTAKIS J. A., GALLMEISTER K. and GREINER C., *Phys. Rev. D*, **104** (2021) 094022.
- [8] NUGARA V., PLUMARI S., OLIVA L. and GRECO V., arXiv:2311.11921 [hep-ph] (2023).
- [9] OLIVA L., FAN W., MOREAU P., BASS S. A. and BRATKOVSKAYA E., *Phys. Rev. C*, **106** (2022) 044910.
- [10] CASSING W. and BRATKOVSKAYA E. L., *Phys. Rev. C*, **78** (2008) 034919.
- [11] CASSING W. and BRATKOVSKAYA E. L., *Nucl. Phys. A*, **831** (2009) 215.
- [12] BRATKOVSKAYA E. L., CASSING W., KONCHAKOVSKI V. P. and LINNYK O., *Nucl. Phys. A*, **856** (2011) 162.
- [13] MORELAND J. S., BERNHARD J. E. and BASS S. A., *Phys. Rev. C*, **101** (2020) 024911.
- [14] SHEN C., QIU Z., SONG H., BERNHARD J., BASS S. and HEINZ U., *Comput. Phys. Commun.*, **199** (2016) 61.
- [15] XU Y., MOREAU P., SONG T., NAHRGANG M., BASS S. A. and BRATKOVSKAYA E., *Phys. Rev. C*, **96** (2017) 024902.
- [16] SONG T., MOREAU P., XU Y., OZVENCHUK V., BRATKOVSKAYA E., AICHELIN J., BASS S. A., GOSSIAUX P. B. and NAHRGANG M., *Phys. Rev. C*, **101** (2020) 044903.
- [17] BANFI A., SALAM G. P. and ZANDERIGHI G., *JHEP*, **06** (2010) 038.
- [18] ORTIZ A., PAIĆ G. and CUAUTLE E., *Nucl. Phys. A*, **941** (2015) 78.
- [19] MALLICK N., SAHOO R., TRIPATHY S. and ORTIZ A., *J. Phys. G*, **48** (2021) 045104.
- [20] ALTMANN J. *et al.*, arXiv:2401.09930 [hep-ex] (2024).
- [21] SOLOVEVA O., MOREAU P. and BRATKOVSKAYA E., *Phys. Rev. C*, **101** (2020) 045203.
- [22] MOREAU P., SOLOVEVA O., OLIVA L., SONG T., CASSING W. and BRATKOVSKAYA E., *Phys. Rev. C*, **100** (2019) 014911.
- [23] BASS S. A. *et al.*, *Prog. Part. Nucl. Phys.*, **41** (1998) 255.
- [24] BLEICHER M. *et al.*, *J. Phys. G*, **25** (1999) 1859.
- [25] DENICOL G. S., JEON S. and GALE C., *Phys. Rev. C*, **90** (2014) 024912.
- [26] BERNHARD J. E., MORELAND J. S. and BASS S. A., *Nat. Phys.*, **15** (2019) 1113.
- [27] SONG H. and HEINZ U. W., *Phys. Rev. C*, **81** (2010) 024905.
- [28] CHATTOPADHYAY C., JAISWAL S., DU L., HEINZ U. and PAL S., *Phys. Lett. B*, **824** (2022) 136820.
- [29] ACHARYA S. *et al.*, *Eur. Phys. J. C*, **79** (2019) 857.
- [30] PRASAD S., MALLICK N., BEHERA D., SAHOO R. and TRIPATHY S., *Sci. Rep.*, **12** (2022) 3917.
- [31] KHUNTIA A., TRIPATHY S., BISHT A. and SAHOO R., *J. Phys. G*, **48** (2021) 035102.
- [32] NASSIRPOUR A., *J. Phys.: Conf. Ser.*, **1602** (2020) 012007.